Archives of Materials Science and Engineering

Volume 96
Issue 1
March 2019
Pages 22-31

International Scientific Journal
published monthly by the
World Academy of Materials
and Manufacturing Engineering

DOI: 10.5604/01.3001.0013.1989

Effect of plastic deformation rate at room temperature on structure and mechanical properties of high-Mn austenitic Mn-Al-Si 25-3-3 type steel

W. Borek [a,*], M. Lis [a], K. Gołombek [a], P. Sakiewicz [a], K. Piotrowski [b]

[a] Institute of Engineering Materials and Biomaterials, Faculty of Mechanical Engineering, Silesian University of Technology, ul. Konarskiego 18a, 44-100 Gliwice, Poland

[b] Department of Chemical Engineering and Process Design, Faculty of Chemistry, Silesian University of Technology, ul. Marcina Strzody 9, 44-100 Gliwice, Poland

* Corresponding e-mail address: wojciech.borek@polsl.pl

ABSTRACT

Purpose: The aim of the paper is to determine influence of plastic deformation rate at room temperature on structure and mechanical properties of high-Mn austenitic Mn-Al-Si 25-3-3 type steel tested at room temperature.

Design/methodology/approach: Mechanical properties of tested steel was determined using Zwick Z100 static testing machine for testing with the deformation speed equal 0.008 s^{-1}, and RSO rotary hammer for testing with deformation speeds of 250, 500 and 1000s^{-1}. The microstructure evolution samples tested in static and dynamic conditions was determined in metallographic investigations using light microscopy as well as X-ray diffraction.

Findings: Based on X-ray phase analysis results, together with observation using metallographic microscope, it was concluded, that the investigated high-Mn X13MnAlSiNbTi25-3-3 steel demonstrates austenitic structure with numerous mechanical twins, what agrees with TWIP effect. It was demonstrated, that raise of plastic deformation rate produces higher tensile strength UTS and higher conventional yield point $YS_{0.2}$. The UTS strength values for deformation rate 250, 500 and 1000 s^{-1} grew by: 35, 24 and 31%, appropriately, whereas in case of $YS_{0.2}$ these were: 7, 74 and 130%, accordingly, in respect to the results for the investigated steel deformed under static conditions, where UTS and $YS_{0.2}$ values are 1050 MPa and 700 MPa. Opposite tendency was observed for experimentally measured uniform and total relative elongation. Homogeneous austenitic structure was confirmed by X-ray diffractometer tests.

Research limitations/implications: To fully describe influence of strain rates on structure and mechanical properties, further investigations specially with using transmission electron microscope are required.

Practical implications: Knowledge about obtained microstructures and mechanical properties results of tested X13MnAlSiNbTi25-3-3 steel under static and dynamic conditions can be useful for the appropriate use of this type of engineering material in machines and equipment susceptible to static or dynamic loads.

Originality/value: The influence of plastic deformation at room temperature under static and dynamic conditions of new-developed high-manganese austenitic X13MnAlSiNbTi25-3-3 steels were investigated.

Keywords: High-Mn steel, TWIP type, Plastic deformation, Twinning, Dynamic deformation, Structure, Mechanical properties

Reference to this paper should be given in the following way:

W. Borek, M. Lis, K. Gołombek, P. Sakiewicz, K. Piotrowski, Effect of plastic deformation rate at room temperature on structure and mechanical properties of high-Mn austenitic Mn-Al-Si 25-3-3 type steel, Archives of Materials Science and Engineering 96/1 (2019) 22-31.

PROPERTIES

1. Introduction

„Steel" is a concept related to iron and carbon alloys. In general this concept is associated with the resistant, rigid material, capable of high loads transmission. It is a group of materials, which practical properties are, however, very diverse. Diversity of these properties is well reflected by so called Ashby Maps [1], as well as dependence presented in Figure 1 [2,3], where changeability of mechanical properties between elongation and tensile strength for different steel brands and groups was proved. Changeability of these properties results from both diversity in chemical composition and different methods applied to form the structure and properties of these steels like thermal treatment, thermal-plastic forming, thermal-chemical treatment and many others. This way, because of diversity of chemical composition, there are distinguished groups and subgroups of these steels. Fundamental steel groups are nonalloyed (carbon) steels and alloy steels [1].

Subgroup of alloy steels covers the ones with raised mechanical strength AHSS (Advanced High-Strength Steels) [4-6]. Within this subgroup one can distinguish three generations. Characteristic of this steel group is unusual dependence between elongation and tensile strength (Fig. 1). This relationship derives from specific structural mechanism, which is activated by plastic deformation. First generation of AHSS steel is represented by low-alloyed steels, like two-phase DP (Dual Phase), multiphase CP (Complex-Phase), MART (Martensitic) steels or steels with phase change TRIP (Transformation Induced Plasticity) [2,5,7-9]. Second generation of AHSS steels is characterized by high fraction of the alloy elements, from 15 to 40%. These are high-Mn steels. This group covers the steels, which plastic deformation mechanisms are as follows: phase change of austenite into martensite ε- and α' TRIP [10-13], plastic deformation induced twinning TWIP (Twinning Induced Plasticity) [11,14-18], as well as plastic deformation induced microbands (microstrips) shearing MBIP (Micro Band Induced Plasticity) [11,19-21]. Third generation of AHSS III steels, characterized by alloy additives content below 10%, are moderate-Mn steels with microstructure composed with many phases, including metastable austenite [22,23].

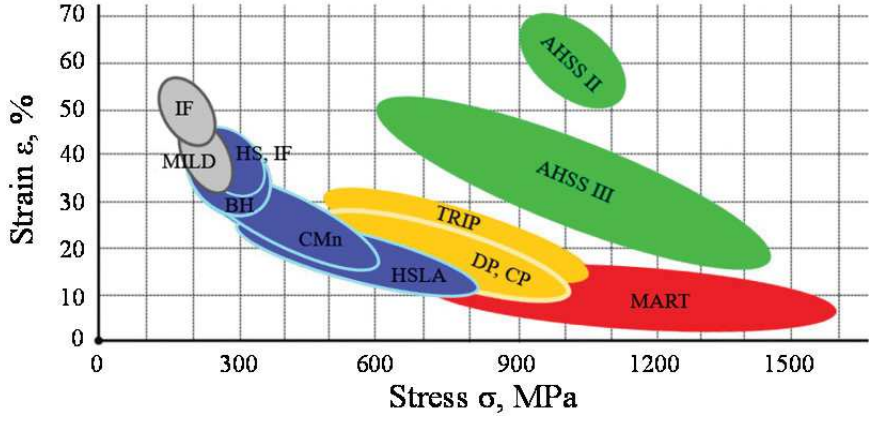

Fig. 1. Comparison of mechanical properties of conventional steels (grey and blue areas on the plot) and advanced high-strength steels AHSS: AHSS I (yellow and red areas), AHSS II and AHSS III (green areas) [2]

The AHSS II steel subgroup is especially interesting because of specific dependency of mechanistic properties, presented in Figure 1. Chemical composition of this subgroup is relatively diverse. Mass fraction of main element of austenitic high-Mn steels, which is manganese, varies from 15 to 35%. Other elements, like aluminium and silica are added in amounts up to 12% Al and up to 4% Si, appropriately, in various combinations. Mass fraction of individual alloy elements, however, determines mechanism (or mechanisms) of plastic steel deformation during its plastic deformation at room temperature. It is the consequence of the fact, that all mentioned alloy additives influence the energy arrangement error (EBU) of austenite, which is dependent on width and number of arrangement errors within crystallographic structure of the steel [24]. It is worth to draw one's attention to the fact, that arrangement errors within crystallographic network result from plastic deformation of the material.

Energy of austenite arrangement error, as mentioned above, is dependent on chemical composition of austenitic high-Mn steels [11,24,25]. Atoms of the alloy additives occupying some locations within crystallographic network of iron, generate within it some defects. This is responsible for the type of induced mechanisms (e.g. slip, twinning) during plastic deformation, thus on the number of arrangement errors and their widths. Increase in concentration of arrangement error network (dislocation density) influences the arrangement error energy value. Decrease of EBU in case of austenite is connected with the growth of arrangement error degree in the crystallographic network, as well as increasing their width, making, that the possibility of deformation occurrence through dislocation climbing or transverse slip is limited [16,24]. This dependence influences the type of plastic deformation mechanism, thus indirectly the steel properties like the ability for energy storage during plastic deformation. This way knowledge of individual effect of alloy elements on mechanistic properties of the steel is necessary for rational selection of chemical composition of the steel and the steel-based constructional elements design.

Main alloy element that is manganese raises the energy arrangement error, simultaneously making, that steel deformed at room temperature becomes more fragile (deteriorates the steel plastic properties). Higher mass fraction of manganese in iron alloys is responsible for stabilization of austenitic structure and formation of mechanical twinnings, especially for Mn exceeding 25 mass % [14,24,26]. Aluminium has the largest influence on EBU. Small addition of this element raises its value significantly. Addition of aluminium in austenitic high-Mn steels improves also plastic properties at room temperature, compensating, to some degree, disadvantageous effect of manganese, which increases the steel brittleness [14,16,19,20,24,27-30]. Other elements lowering the EBU and improving mechanical properties through solution's hardening (consolidation) of austenitic high-Mn steels are silica and carbon. Moreover, carbon lowers necessary mass fraction of manganese, required for manufacturing of stable austenitic structure [14,27,31-33]. In the steels containing comparable mass fraction of aluminium and silica, advantageous influence on plasticity is observed when Mn content is lower [34]. Microadditives, like Ti or Nb, form in steels carbides, nitrides, as well as carbidenitrides because of high their affinity to carbon and nitrogen. These compounds limit grains growth within the steel, decrease EBU, as well as improve strength properties of these steels [27,35].

Based on numerous tests and scientific reports for this group of austenitic high-Mn steels, three characteristic ranges for the arrangement error energy value were assumed, as well as the corresponding ranges of appropriate mechanisms of plastic deformation at room temperature [9,20,24,27,36,37]. First of them was determined for austenitic high-Mn steels demonstrating TRIP effect. In this case the following relation EBU $\leq$20 mJ/m^2 is valid. Concentrations of main alloy elements for austenitic high-Mn steels varies in this range from 15 to 22 mass % of manganese, up to 3 mass % of aluminium and silica, as well as from 0.05 to 0.15 mass % of carbon. In the next range there are austenitic high-Mn steels demonstrating TWIP effect. This effect is observed for the following combination of element concentrations: from 20 to 30 mass % of manganese, from 3 to 5 mass % of aluminium, up to 3 mass % of silica and from 0.02 to 0.65 mass % of carbon. Energy of arrangement error for this range varies from 20 to 60 mJ/m^2. Last type of austenitic high-Mn steel is the group demonstrating hardening (consolidation) effect in MBIP. For these steels EBU value is $\geq$ 60 mJ/m^2. Element concentrations vary: from 18 to 35 mass % of manganese, from 8 to 12 mass % of aluminium, from 3 to 6 mass % of silica and from 0.5 to 1.3 mass % of carbon.

Austenitic high-Mn steels of TWIP type demonstrate intensive mechanical twinning induced by plastic deformation at room temperature. Intensity of twins generation in the grains depends on dislocation density and single dislocation errors. Thus, at room temperature, it demonstrates unusual properties, like [16,24,38] high tensile strength at even high total elongation, thus high ability for impact energy absorbing in result of its „consumption" for crystallographic structure spatial arrangement.

In austenitic high-Mn steels of TWIP type deformation rate influences the change of yield point value. It grows with increase in deformation dynamics. A characteristic of

deformation with high rate is occurrence of wave phenomenon and inertia forces in deforming material. In this case the time, in which the material undergoes loading is so short, that energy is accumulated in its part only, while other material volume remains free from acting load. From this reason in deforming material there is generated some form of a wave of relocating tension and deformation, with some defined rate. It means, that during plastic deformation, generated twins are initiated in the subsequent grains, starting from the place of sample break. Thus hardening (consolidation) and deformation are local phenomena, thus intensity of twins generation within whole volume is different [9,24]. One should take attention, that parameters of deformation/tensile strength, like deformation rate, demonstrate nonlinear character (these values, for different deformation rates raise and drop), simultaneously maintaining ability for hardening (consolidation) and absorbing of energy during deformation, despite increasing plastic deformation rate [39]. The hardening (consolidation) effect, thus growth of plasticizing tension value, for austenitic high-Mn steels of TWIP type is observed only under conditions of dynamic plastic deformation [27]. Thus these steels find themselves useful in constructional elements, which must demonstrate high tensile properties under conditions of dynamic plastic deformation, where deformation rate exceeds 1 s^{-1}. Good example may be automotive industry, which is especially interested in development of this steel subgroup in respect to the production of elements responsible for transmission and absorbing of impact energy during e.g. road accident.

Additional hardening (consolidation) effect in austenitic high-Mn steels of TWIP type is dynamic deformation ageing, which relies on blocking of unconstrained movement of the dislocation through presence of Cottrel's atmospheres and interstitial atoms present in the close neighbourhood of dislocation core. This effect is especially observable during the dynamic deformation tests. It is externally observed as yield point growth in the investigated steel [40,41].

2. Material

The austenitic high-Mn X13MnAlSiNbTi25-3-3 steel, of chemical composition presented in Table 1, was tested. Chemical composition of the steel was appropriately selected, to provide single-phase austenitic structure and mechanism of intensive twinning during plastic deformation at room temperature.

Table 1.
Chemical composition of high-manganese X13MnAlSiNbTi25-3-3 steel, mass fraction

C	Mn	Si	Al	Nb	Ti	Ce	Nd	La	S	P	N, ppm	O, ppm
0.13	25.1	3.5	3.3	0.05	0.018	0.013	0.005	0.003	0.002	<0.002	28	<6

3. Research methods

Breaking of the samples, made of austenitic high-Mn X13MnAlSiNbTi25-3-3 steel, were done using rotary hammer, WPM Leipzig. Deformation speeds were 250, 500 and 1000 s^{-1}. Samples were fixed and stiffened with one side, inside the measuring bar hole, on the other side in the hole of lower holder – anvil. In next stage flywheel was accelerated up to the assumed rotational speed. Then the hammer's claw was released, which stroke directly the anvil resulting in sample breaking. The break force was determined based on resulting springy wave, which was measured with resistant strain gauge fixed to measuring bar. Deformation rate was determined with fixed to end of the encoder shaft's pivot. For the tests flat samples were used, of rectangular cross section, of dimensions presented in Figure 2.

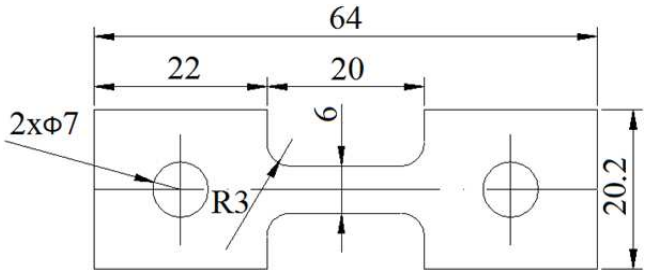

Fig. 2. The shape and dimensions of the samples used for testing in dynamic conditions

Static tensile tests were carried out on Zwick Z100 static testing machine with the deformation speed of the tested 0.008 s^{-1}. Obtained results were analysed with testXpert II software. Samples provided for the tests were flat and were prepared according to PN-EN 10002-1 norm.

Phase X-ray analyses were done with X-ray diffractometer XPert PRO, Panalytical. For the determination of phase composition of original sample and sample after breaking, filtered beam of X-ray radiation of wavelength $K_{\alpha 1}$ $\lambda = 1.78897$nm was used, emitted by Cu X-ray tube supplied by electric current of intensity 30 mA and voltage 40 kV. Measurement range of 2θ angle varied from 35 to 130°. Tests were done with the step method, with step 0.05°. The diffraction patterns produced were analysed with the use of International Centre for Diffraction Data (ICDD) library.

Cut fragments of breaked samples were inclused in a resin, in the manner making further metallographic microscope observations of fractures and structural changes possible. Sample fragments were oriented in parallel in respect to their axes. The images were done using optical microscope Zeiss AxioObserver. Prepared metallographic specimens were etched with 10% nitric acid, digested in ethyl alcohol. Observations with metallographic microscope were done for identification of structural changes after plastic deformation of the material.

4. Results

The resulting measurement data after breaking tests with rotary hammer were transformed to the form making determination of mechanical properties of austenitic high-Mn X13MnAlSiNbTi25-3-3 steel possible. Test results in a form of numerical values obtained under the static and dynamic deformation conditions are presented in Table 2. The effect of strain hardening demonstrates as the significant growth of tensile properties during cold plastic deformation.

The diagrams illustrating the corresponding plastic deformation tests at room temperature, in static tensile test, as well as breaking under dynamic conditions, are presented in Figure 3. These suggest that with the increase in deformation rate total elongation decreases, however significant growth of yield point is also observed. Dynamic deformation conditions cause increase of tensile properties of the analysed steel. This may indicate a consolidation of the material in effect of plastic deformation mechanism (TWIP).

Table 2.
The results of strength tests, static tensile tests and breaking at dynamic conditions (UTS – ultimate tensile strength, $YS_{0.2}$ – yield point, ε_{un} – uniform relative elongation, ε_t – total relative elongation)

	Deformation rate			
	0.008 s^{-1}	250 s^{-1}	500 s^{-1}	1000 s^{-1}
$YS_{0.2}$, MPa	700	750	1220	1610
UTS, MPa	1050	1420	1300	1380
ε_{un}, -	0.29	0.25	0.24	0.21
ε_t, -	0.32	0.27	0.26	0.24

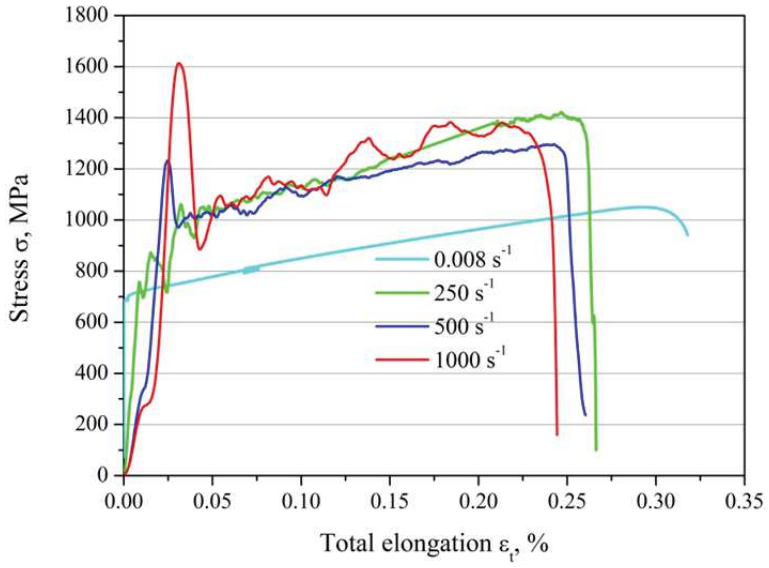

Fig. 3. Representative chart – static and dynamic tests of samples made of high-Mn austenitic steel X13MnAlSiNbTi25-3-3

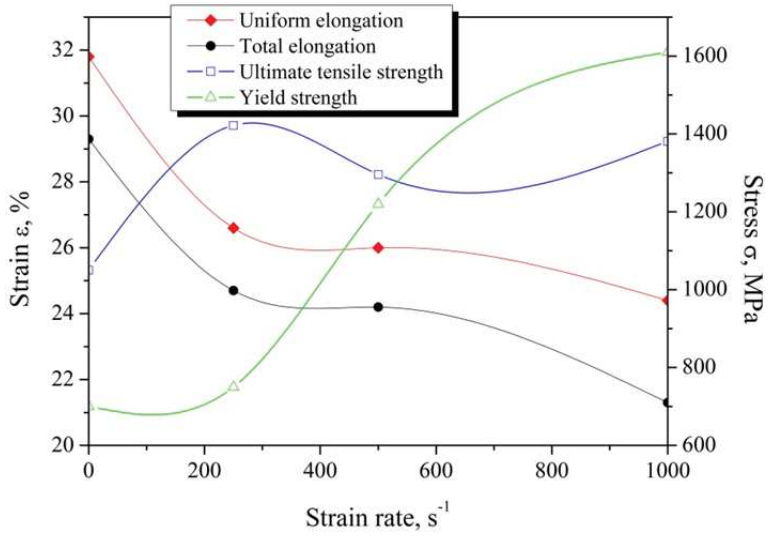

Fig. 4. Change of mechanical properties of high-Mn austenitic X13MnAlSiNbTi25-3-3 steel tested for selected plastic deformation strain rates

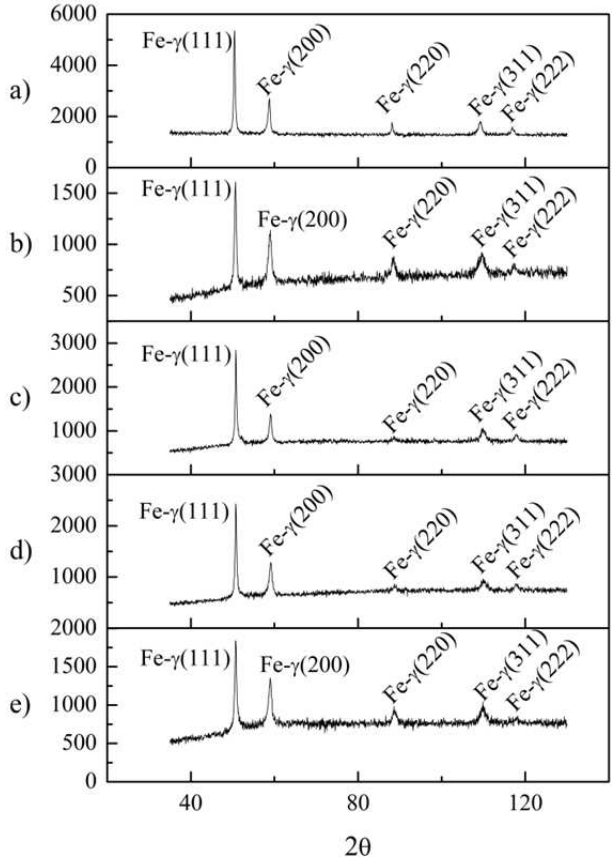

Fig. 5. X-ray diffraction patterns of high-Mn austenitic steel X13MnAlSiNbTi25-3-3: a) initial state of the sample; b) sample tensile under static conditions; c) sample broken under dynamic conditions, with strain rate 250 s^{-1}; d) sample broken under dynamic conditions, with strain rate 500 s^{-1}; e) sample broken under dynamic conditions, with strain rate 1000 s^{-1}

Changes in the considered properties are graphically presented in Figure 4, which demonstrates dependency of mechanical properties on plastic deformation rate at room temperature, starting from static tensile test with the rate of 0.008 s^{-1}, up to dynamic breaking with the rate of 1000 s^{-1}. Phase analysis, made with the use of X-ray diffractometer, was used for the verification of main deformation mechanism. High-Mn steels of TWIP type after plastic deformation at room temperature should demonstrate presence of austenite phase in the whole material volume. Based on the obtained diffraction patterns it was concluded, that investigated high-Mn steel X13MnAlSiNbTi25-3-3 shows homogeneous austenite structure (Fig. 5a). Varying plastic deformation rate did not cause changes within phase structure of the analysed steel (Fig. 5b-e).

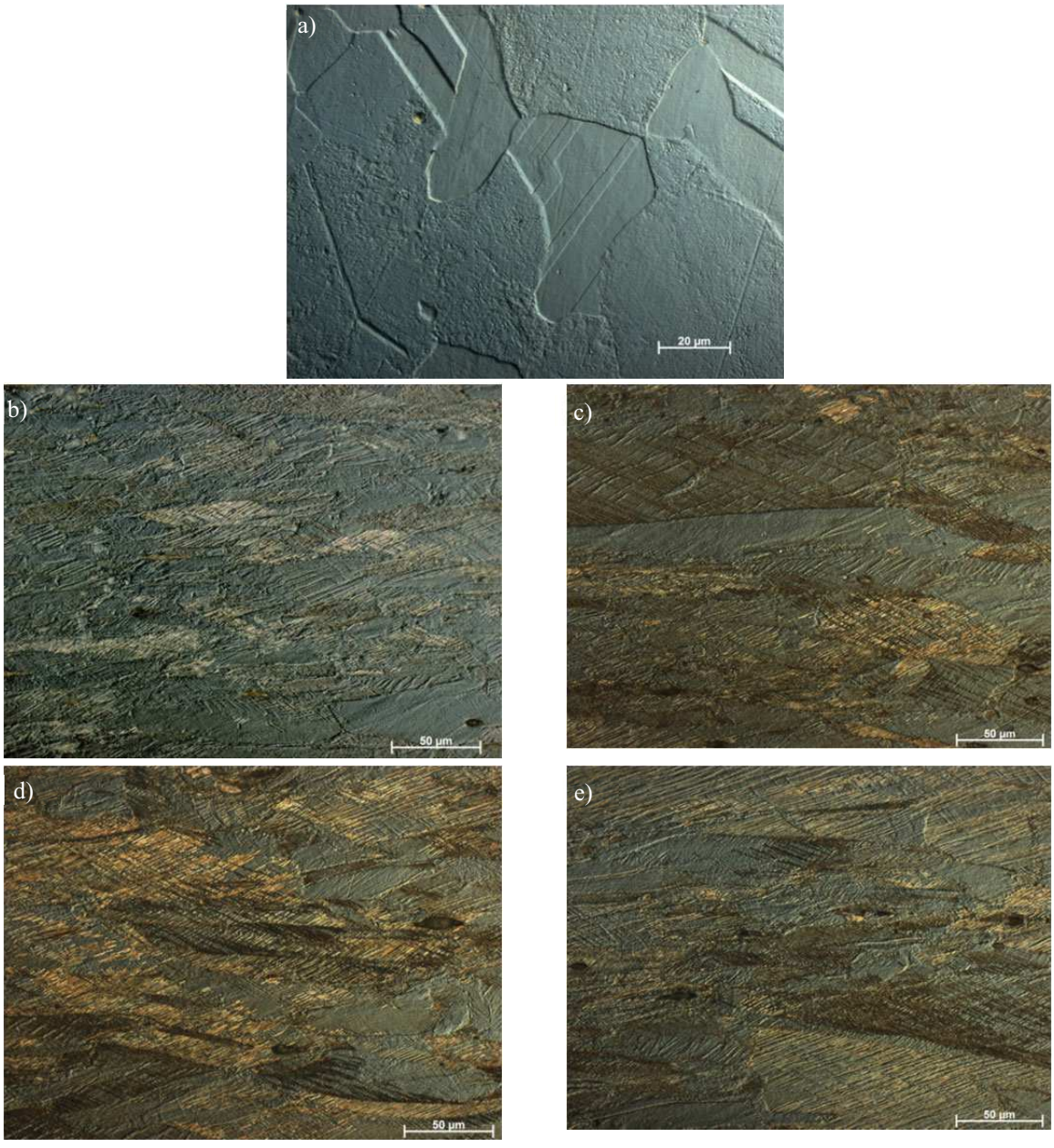

Fig. 6. Structure of high-Mn austenitic X13MnAlSiNbTi25-3-3 steel, a) initial state of the sample; b) sample tensile under static conditions; c) sample broken under dynamic conditions, with strain rate 250 s^{-1}; d) sample broken under dynamic conditions, with strain rate 500 s^{-1}; e) sample broken under dynamic conditions, with strain rate 1000 s^{-1}

Selected regions in structures of austenite high-Mn steel samples tested, which were subject of observations using metallographic microscope, are presented in the form of images in Figure 6. Figure 6a represents structure of austenite high-Mn steel X13MnAlSiNbTi25-3-3 in original state. This original structure is characterized by occurrence of numerous twins annealing, which proceed within single grains structures. Structure of the investigated steel after plastic deformation at room temperature under static conditions is presented in Figure 6b. Next images present structures of analysed steel after plastic deformation under dynamic conditions of breaking, with rates of: 250 s^{-1} (Fig. 6c), 500 s^{-1} (Fig. 6d), 1000 s^{-1} (Fig. 6e). Structure of tested steel after deformation, both under static and dynamic conditions, is characterized by presence of slip bands and mechanical twins. Mechanical twins are observed as narrow bands crossing entirely or partially austenite grains. Mechanical twins visible in the images cross also in two slip systems. The difference in length of generated mechanical twins, in relation to static tensile tests and dynamic breaking tests, were identified experimentally. It was concluded, that increase in plastic deformation rate influences the length of generated mechanical twins advantageously.

5. Conclusions

Based on X-ray phase analysis results, together with microstructure observation using metallographic microscope, it was concluded, that the investigated high-Mn X13MnAlSiNbTi25-3-3 steel demonstrates austenitic structure with numerous mechanical twins, what agrees with TWIP effect. Increase in its tensile properties, like tensile strength and yield point, results from deformation-induced mechanical twinning. It was demonstrated, that raise of plastic deformation rate produces higher tensile strength UTS and higher conventional yield point $YS_{0.2}$ (Table 2). The UTS strength values for deformation rate 250, 500 and 1000 s^{-1} grew by: 35, 24 and 31%, appropriately, whereas in case of $YS_{0.2}$ these were: 7, 74 and 130%, accordingly, in respect to the results for the investigated steel deformed under static conditions, where UTS and $YS_{0.2}$ values are 1050 MPa and 700 MPa. Opposite tendency was observed for experimentally measured uniform and total relative elongation. With the deformation rate increase, plastic properties decrease. The largest total relative elongation corresponded to the tensile test under static conditions, which is 0.32. The lowest value was 0.24 for deformation rate 1000 s^{-1}. It was observed, that the character of total relative elongation decrease is nearly linear (Fig. 4). Homogeneous austenitic structure was confirmed by X-ray diffractometer tests. This way it may be concluded, that raise of deformation rate, as well as accompanying deformation hardening (consolidation), does not influence the change in phase structure of the investigated austenitic high-Mn steel (Fig. 5). The observations using metallographic microscope made evaluation of the effect of plastic deformation on structure of austenitic high-Mn steel possible where mechanical twins were observed (Fig. 6). The mechanical twins generated cross in two deformation systems. Presence of slip bands was identified. Based on changes in grain dimensions, the direction of single-axis breaking force action was noticed. Based on the research done it was concluded, that the austenite high-Mn X13MnAlSiNbTi25-3-3 steel may be used as constructional element working in devices, machines, tools, instruments, where raised mechanical strength under dynamic conditions of deformation is required, providing safety of use in a given application.

References

[1] L.A. Dobrzański, Fundamentals of materials science and metallurgy, WNT, Warszawa, 2003 (in Polish).
[2] M. Ambroziński, S. Polak, Z. Gronostajski, R. Kuziak, W. Chorzępa, M. Pietrzyk, Numerical simulation of crash test accounting for the strain hardening in the manufacturing process of energy-absorbing part in the car body, Mechanic 88/2 (2015) 92-97 (in Polish).
[3] L. Sozańska-Jędrasik, J. Mazurkiewicz, W. Borek, K. Matus, Carbides analysis of the high strength and low density Fe-Mn-Al-Si steels, Archives of Metallurgy and Materials 63/1 (2018) 265-276.
[4] R. Kuziak, R. Kawalla, S. Waengler, Advanced high strength steels for automotive industry, Archives of Civil and Mechanical Engineering 8/2 (2014) 103-117.
[5] M. Askari-Paykani, H.R. Shahverdi, R. Miresmaeili, First and third generations of advanced high-strength steels in a FeCrNiBSi system, Journal of Materials Processing Technology 238 (2016) 383-394.
[6] J.-H. Schmitt, T. Iung, New developments of advanced high-strength steels for automotive applications, Comptes Rendus Physique 19/8 (2018) 641-656.
[7] B. Fu, W.Y. Yang, Y.D. Wang, L.F. Li, Z.Q. Sun, Y. Ren, Micromechanical behavior of TRIP-assisted multiphase steels studied with in situ high-energy

X-ray diffraction, Acta Materialia 76 (2014) 342-354.
[8] G. Rosenberg, I. Sinaiová, Ľ. Juhar, Effect of microstructure on mechanical properties of dual phase steels in the presence of stress concentrators, Materials Science and Engineering A 582 (2013) 347-358.
[9] J. Senkara, Contemporary car body steels for automotive industry and technological guidelines of their pressure welding, Welding Review 81/11 (2009) 3-7.
[10] T.Y. Liu, P. Yang, L. Meng, F.Y. Lu, Influence of austenitic orientation on martensitic transformations in a compressed high manganese steel, Journal of Alloys and Compounds 509/33 (2011) 8337-8344.
[11] K.T. Park, G. Kim, S.K. Kim, S.W. Lee, S.W. Hwang, C.S. Lee, On the transitions of deformation modes of fully austenitic steels at room temperature, Metals and Materials International 16/1 (2010) 1-6.
[12] A. Tomaszewska, Research of properties of X20MnAl17-3 steel, Metallurgist 78/8 (2011) 674-677 (in Polish).
[13] X. Li, L. Chen, Y. Zhao, R.D.K. Misra, Influence of manganese content on ε-/α′-martensitic transformation and tensile properties of low-C high-Mn TRIP steels, Materials and Design 142 (2018) 190-202.
[14] L. Chen, Y. Zhao, X. Qin, Some aspects of high manganese twinning-induced plasticity (TWIP) steel, a review, Acta Metallurgica Sinica (English Letters) 26/1 (2013) 1-15.
[15] S. Curtze, V. Kuokkala, Dependence of tensile deformation behavior of TWIP steels on stacking fault energy, temperature and strain rate, Acta Materialia 589/5 (2010) 5129-5141.
[16] B.C. De Cooman, K.G. Chin, J. Kim, High Mn TWIP steels for automotive applications, in: M. Chiaberge (Ed.), New Trends and Developments in Automotive System Engineering, No. 1, Intech, Rijeka, 2011, 101-128.
[17] L.A. Dobrzański, W. Borek, J. Mazurkiewicz, Influence of high strain rates on the structure and mechanical properties of high-manganese austenitic TWIP-type steel, Materialwissenschaft Und Werkstofftechnik 47/5-6 (2016) 428-435.
[18] W. Borek, T. Tański, Z. Jonsta, P. Jonsta, L. Cizek, Structure and mechanical properties of high-Mn TWIP steel after their thermo-mechanical and heat treatments, Proceeedings of the 4th International Conference on Metallurgy and Materials "METAL 2015", 2, 2015, 307-313.
[19] J.D. Yoo, K.-T. Park, Microband-induced plasticity in a high Mn-Al.-C light steel, Materials Science and Engineering A 496/1 (2008) 417-424.
[20] S. Chen, R. Rana, A. Haldar, R.K. Ray, Current state of Fe-Mn-Al-C low density steels, Progress in Materials Science 89 (2017) 345-391.
[21] J. Moon, S.J. Park, J.H. Jang, T.H. Lee, C.H. Lee, H.U. Hong, H.N. Han, J. Lee, B.H. Lee, C. Lee, Investigations of the microstructure evolution and tensile deformation behavior of austenitic Fe-Mn-Al-C lightweight steels and the effect of Mo addition, Acta Materialia 147 (2018) 226-235.
[22] A. Grajcar, R. Kuziak, W. Zalecki, Third generation of AHSS with increased fraction of retained austenite for the automotive industry, Archives of Civil and Mechanical Engineering 12/3 (2012) 334-341.
[23] W.W. Sun, Y.X. Wu, S.C. Yang, C.R. Hutchinson, Advanced high strength steel (AHSS) development through chemical patterning of austenite, Scripta Materialia 146 (2018) 60-63.
[24] M.B. Jabłońska, Structure and properties of austenitic high-manganese steel reinforced due to mechanical twins in dynamic deformation processes, Silesian University of Technology Publishing House, Gliwice, 2016 (in Polish).
[25] O. Bouaziz, S. Allain, C.P. Scott, P. Cugy, D. Barbier, High manganese austenitic twinning induced plasticity steels: A review of the microstructure properties relationships, Current Opinion in Solid State and Materials Science 15/4 (2011) 141-168.
[26] S.W. Bhero, B. Nyembe, K. Lentsoana, Common failures of hadfield steel in application, Proceednigs of the International Conference on Mining, Mineral Processing and Metallurgical Engineering "ICMMME'2014", Johannesburg, 2014, 17-19.
[27] S. Kołodziej, Influence of martensitic transformation on the structure and anisotropic properties of high manganese TWIP plastically deformable steels, Silesian University of Technology, Gliwice, 2016 (in Polish).
[28] S. Wenwen, I. Tobias, W. Bleck, Control of strain hardening behavior in high-Mn austenitic steels, Acta Metallurgica Sinica (English Letters) 27/3 (2014) 546-555.
[29] A. Bronz, V. Deminskaya, L. Kaputkina, V. Kindop, D. Kremyansky, Structure and strength cast high aluminum and manganese of iron alloys with a high carbon content, National University of Science and Technology, 36-39.
[30] K. Hansoo, S. Dong-Woo, J.K. Nack, Fe-Al-Mn-C lightweight structural alloys: a review on the microstructures and mechanical properties, Science and Technology of Advanced Materials 14/1 (2013) 14205.

[31] M.B. Jabłońska, A. Śmiglewicz, G. Niewielski, The effect of strain rate on the mechanical properties and microstructure of the high-Mn steel after dynamic deformation tests, Archives of Metallurgy and Materials 60/2 (2015) 577-580.
[32] E. Mazancová, I. Schindler, K. Mazanec, Stacking fault energy analysis from point of view of plastic deformation response of the TWIP and TRIPLEX alloys, Proceedings of the 18th International Conference on Metallurgy and Materials "Metal 2009", Hradec nad Moravicí, 2009.
[33] X. Tian, Y. Zhang, Effect of Si content on the stacking fault energy in γ-Fe-Mn-Si-C alloys: Part II. Thermodynamic estimation, Materials Science and Engineering A 516/2 (2009) 78-83.
[34] O. Grässel, L. Krüger, G. Frommeyer, L. Meyer, High strength Fe–Mn–(Al, Si) TRIP/TWIP steels development – properties – application, International Journal of Plasticity 16/10 (2000) 1391-1409.
[35] L.A. Dobrzański, W. Borek, J. Mazurkiewicz, Mechanical properties of high-Mn austenitic steel tested under static and dynamic conditions, Archives of Metallurgy and Materials 61/2 (2016) 725-730.
[36] A. Śmiglewicz, M.B. Jabłońska, K. Rodak, Stacking fault energy and mechanical twinning in the high-manganese X30MnAlSi26-4-3 steel, Metallurgist 82/8 (2015) 472-474 (in Polish).
[37] K.-T. Park, K.G. Jin, S.H. Han, S.W. Hwang, K. Choi, C.S. Lee, Stacking fault energy and plastic deformation of fully austenitic high manganese steels: Effect of Al addition, Materials Science and Engineering A 527/16 (2010) 3651-3661.
[38] L.A. Dobrzański, A. Grajcar, W. Borek, Microstructure evolution of high-manganese steel during the thermomechanical processing, Archives of Materials Science and Engineering 37/2 (2009) 69-76.
[39] G. Frommeyer, U. Brüx, P. Neumann, Supra-ductile and high-strength manganese-TRIP/TWIP steels for high energy absorption purposes, ISIJ International 43/3 (2003) 438-446.
[40] P.S. Kusakin, R.O. Kaibyshev, High-Mn twinning-induced plasticity steels: Microstructure and mechanical properties, Reviews on Advanced Materials Science 44/4 (2016) 326-360.
[41] S.G. Hong, S.B. Lee, Mechanism of dynamic strain aging and characterization of its effect on the low-cycle fatigue behavior in type 316L stainless steel, Journal of Nuclear Materials 340/2 (2005) 307-314.